Molecular & Cellular Biomechanics 2025, 22(3), 1359.
https://doi.org/10.62617/mcb1359

Article

Design of 2D gimbal face localization and fatigue driving detection system

Peng Zhao, Yichong Jia*, Yongming Zhang

Xinjiang Institute of Technology, School of Mechanical and Electrical Engineering, Aksu 843100, China
*** Corresponding author:** Yichong Jia, jiayichong88@163.com

CITATION

Zhao P, Jia Y, Zhang Y. Design of 2D gimbal face localization and fatigue driving detection system. Molecular & Cellular Biomechanics. 2025; 22(3): 1359. https://doi.org/10.62617/mcb1359

ARTICLE INFO

Received: 13 January 2025
Accepted: 17 February 2025
Available online: 26 February 2025

Abstract: Aiming at the traditional fatigue driving detection system with a single function, unable to locate the face, greatly affected by external lighting factors and high hardware requirements, this design proposes a system that uses OpenMV equipped with a CMOS camera as the main controller, recognizes the face contour by using Haar classifiers, and controls the two-dimensional gimbal to realize the face localization function, with the MCU as the slave, and utilizes the MCU to read the blinking frequency per time unit to determine the fatigue driving. The microcontroller is the slave, using the microcontroller to read the blinking frequency captured by OpenMV per unit time to judge the fatigue driving, when the blinking frequency is higher than 30 times/min, the microcontroller triggers the sound and light alarm. At the same time, the neck and waist signal analysis module is added to collect more comprehensive driver fatigue information. For complex road conditions such as sharp curves, up and down slopes, the microcontroller can pre-judge in advance through the positioning module to remind the driver in the form of alarm. The experiment proves that the system adopts lightweight design scheme, applicable to the field of in-vehicle electronics, both with the advantages of diversified functions, high measurement accuracy, intuitive display, stable operation, etc. The combination of 2D PTZ face localization and fatigue driving detection in the mode of master-slave improves the real-time and robustness of the control system, which is useful for the improvement of fatigue driving detection by using machine vision.

Keywords: 2D gimbal; face localization; fatigue driving; Haar classifier; blink frequency

1. Introduction

If the method of PERCLOS is used in the detection of unsafe driving, there is a certain monitoring blind spot due to the influence of the driver's head swing, and the amount of data combined with body movements such as smoking and yawning is often very large, and it is difficult to run the analysis program on a PC in real time in the vehicle embedded electronic equipment. Relying on PERCLOS to identify fatigue driving, there is a better recognition accuracy for heavy fatigue and a poorer recognition accuracy for shallow fatigue; there is also a slow recognition of fatigue driving, reminders are not timely, leaving the driver's response time is too short; by the driver's individual differences in the impact of the threshold of these indicators is also to be carried out to determine the threshold of the more practical driving tests. Neck and lumbar muscle fatigue is a common problem during long driving, especially the fatigue of the trapezius muscle in the neck and the lumbar erector ridge muscle will directly affect the driver's posture and reaction ability. Through the introduction of EMG signal analysis, the system can more comprehensively evaluate the fatigue state of the driver from the perspective of muscle activity, making up for the shortage of relying on visual information only. Zhang et al. studied sEMG and accelerometer signals and used multimodal fusion convolutional neural networks to improve the accuracy of cross-individual upper limb motion classification. By introducing the two-flow convolution model, the common information between different individuals can be extracted, which significantly improves the classification performance, especially under the training of multiple individual data, the performance is better than the traditional single signal input model. This method effectively overcomes the problem of data distribution differences among individuals [1]. Salah et al. proposed a method of combining event-driven neuromorphic vision sensors with traditional vision techniques to improve the speed and accuracy of hole and slot detection. The introduction of motion compensation and mean offset clustering algorithms can reduce the uncertainty of sensor output and significantly improve the detection accuracy and response speed, demonstrating the advantages of multi-modal technology in the manufacturing process [2]. Therefore, this paper proposes a lightweight fatigue driving detection scheme applicable to the field of in-vehicle electronics, using the OpenMV equipped with CMOS camera OV5640 as the main controller, combined with the slave microcontroller, the main controller camera using Haar classifier and PID control algorithms to achieve face feature extraction and control the steering of the 2D gimbal, to achieve the function of face localization; the slave machine unit of time The slave machine reads the blinking frequency of the host machine to determine whether it is fatigue driving and provides driving road condition information. Using the neck and waist signal analysis as an auxiliary technology to analyze the driver's state more comprehensively. Adopting the master-slave mode improves the data acquisition efficiency of the master controller and makes up for the problem of limited hardware resources and low real-time performance of the in-vehicle electronic system.

2. System architecture analysis

The overall scheme of the face localization and fatigue driving detection system is shown in **Figure 1**, the whole system consists of an image recognition and processing module OpenMV, a 2D gimbal, a MSP430F5529 microcontroller, an alarm module, a localization module, a storage module, and a display module, OpenMV carries a camera component, and the face detection is done by using a Haar Cascade feature detector on the image to recognition, which can acquire the driver's face image data, analyze the captured face, drive the servo, and control the gimbal to track the face. According to the face using the Haar operator of the eye to locate the human eye, determine the position of the pupil through the recognition of the color depth, combined with the microcontroller timer real-time calculation of the driver's blinking frequency and determine whether the driver is fatigued driving [3–5]. The Haar classifier has excellent performance in complex environments, especially when the driver's head is moving quickly and glasses are worn. By adjusting the image resolution and frame rate, the system can effectively track the face in rapid motion, ensuring that the head can be adjusted in time to maintain face positioning. In addition, the Haar classifier effectively deals with lens reflection and light interference through dynamic exposure and gain adjustment, improving the recognition accuracy under complex lighting conditions. Combined with optimization strategies, the system operates stably in a variety of complex environments, ensuring accurate face positioning and fatigue monitoring. OpenMV communicates with the MSP430F5529 microcontroller through the serial port to transmit the driver's abnormal driving signals [6–9]. The microcontroller uses GPS or BDS to obtain the current location information through the positioning module, and the storage module stores the location information for traffic accidents that are prone to occur, and the microcontroller combines the storage information and the positioning information to warn the driver in the process of driving on special road sections through the alarm module.

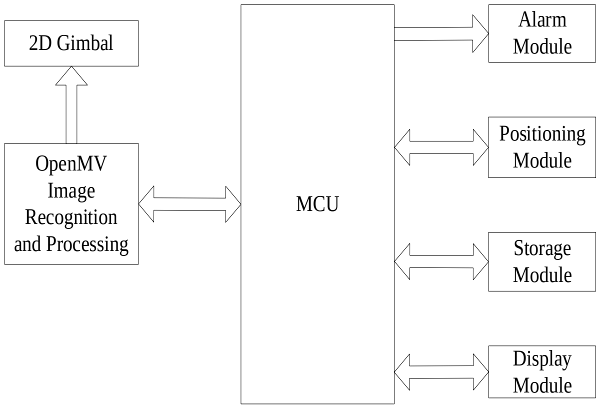

Figure 1. System architecture diagram.

3. 2D gimbal control and fatigue detection algorithm

3.1. Face recognition algorithm

Common face detection methods include Haar, Hog, CNN, SSD, MTCNN, etc [10–12]. Haar is fast and suitable for in-vehicle electronic systems with small computing power. In this design, the Haar feature classifier on OpenMV is used to quickly recognize faces within the field of view and obtain the X, Y-axis coordinates of the faces [13–16]. The specific face detection effect is shown in **Figure 2**.

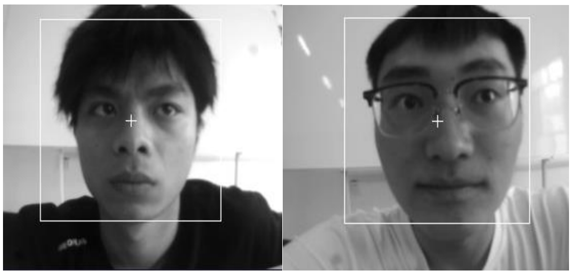

Figure 2. Effect of face detection.

3.2. Human eye recognition algorithm

In the application environment inside a car, the driver's face position is relatively fixed, so the Haar operator for faces can be utilized to quickly recognize the driver's face [17–20]. Then the Cascade classifier of Haar features is utilized to detect the driver's eye position, thus marking the eye region and obtaining the pupil coordinates [21,22]. **Figure 3** shows the recognition of human eyes in different states.

Figure 3. Human eye recognition without and with glasses.

3.3. 2D gimbal control algorithm

The 2D gimbal consists of a combination of two servos, equipped with OpenMV to enable the camera to achieve 360° rotation in the horizontal direction and 180° rotation in the vertical direction. Its physical assembly diagram is shown in **Figure 4**.

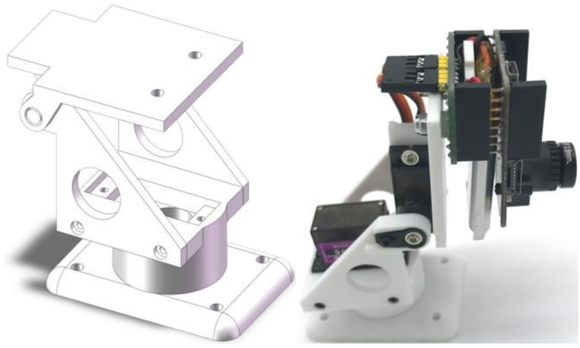

Figure 4. 2D gimbal 3D drawing and physical drawing.

Using OpenMV to obtain the X and Y axis coordinates of the target object, calculate the coordinates of the center point of the detection frame, and when the offset of the center point position exceeds the pre-set threshold, get the offset and control the direction of the gimbal according to its magnitude, so that the center of the camera's field of view is always the same as the geometric center of the human face [23,24]. Under the pixel coordinate system, judging the relationship between the center of the object tracked by the gimbal and the rotation of the gimbal, the steering direction of the gimbal can be classified into the following eight cases, as shown in **Figure 5**.

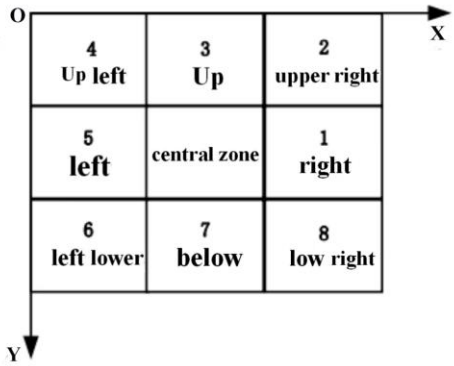

Figure 5. Direction of motion of the head.

PID algorithms are divided into two types: positional and incremental. The integral link of positional PID is to integrate the deviation of the whole control system, and each output value obtained is closely related to the motion state of the object in the previous frame, which is easy to cause integral saturation. The output of incremental PID algorithm is related to the deviation value of three consecutive frames, and the final output value is obtained through the comparison of three moments, which prevents the error from accumulating too much and affects the control accuracy [25,26]. Therefore, this design adopts the incremental PID algorithm to control the gimbal without considering the integral saturation, which simplifies the software design, and its incremental flowchart is shown in **Figure 6**.

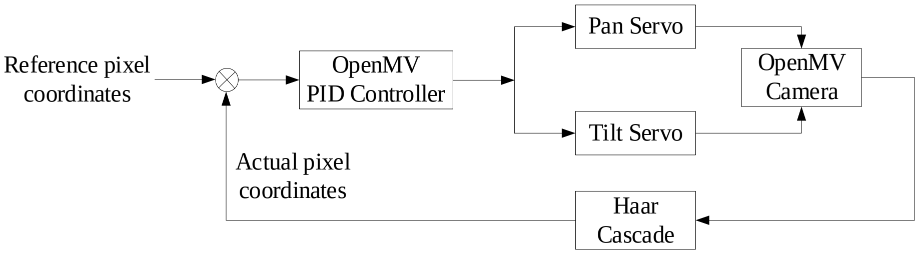

Figure 6. Head steering PID control schematic diagram.

PID parameters should be adjusted according to the dynamic characteristics of the system. The proportional gain determines the influence of the current error on the control output. Choosing the right Kp value is the key to ensure the fast and accurate positioning of the PTZ. Integral control acts on the cumulative error and can eliminate the steady-state error of the system. Therefore, when selecting Ki values, it is necessary to ensure that the system can maintain stability in long-term operation and that errors will not accumulate excessively. Differential control acts on the rate of error change and can effectively suppress the oscillation and overshoot of the system. By calculating the error change of the first few frames, incremental PID avoids the integral saturation problem caused by the integral link in the traditional PID, so as to improve the real-time and stability of the control. When tuning parameters, the proportional gain is set to 5, and the integral gain and differential gain are initially set to 0. Increase the Kp value to make the system respond faster until the head quickly approaches the target face without significant oscillations. Adjust the Kd value to reduce oscillations and ensure smooth system transition.

3.4. Fatigue detection algorithm

3.4.1. PERCLOS algorithm

Eye changes are an effective indicator of fatigue status, and the PERCLOS algorithm detects fatigue status by calculating the ratio of a driver’s eyes closed to a specific degree over a period of time. Several common standards for this algorithm include P70, P80, and EM, and the specific method is to calculate the ratio of the time in which the eye closure ratio exceeds 70%, 80%, and 50% to the total observation time in a specific time interval [27,28].

3.4.2. Blink frequency algorithm

The blink frequency algorithm determines the number and frequency of blinks by comparing the pupil area of the driver in normal and fatigued driving conditions. The method recognizes each blinking action and accumulates it. Taking the P80 standard as an example, only one blink is recorded when the degree of eye closure reaches or exceeds 80%, without the need to accurately grasp the closure time, which reduces the requirements of hardware configuration and is more suitable for application in vehicle electronic systems.

The detection algorithm, as illustrated in **Figure 7**, is also based on the P80 standard, which records only one blink when the eye closure is at or above 80%, thus calculating the total number of blinks in a time period, c. Let f be the blink frequency, which can be calculated from the corresponding Equation (1).

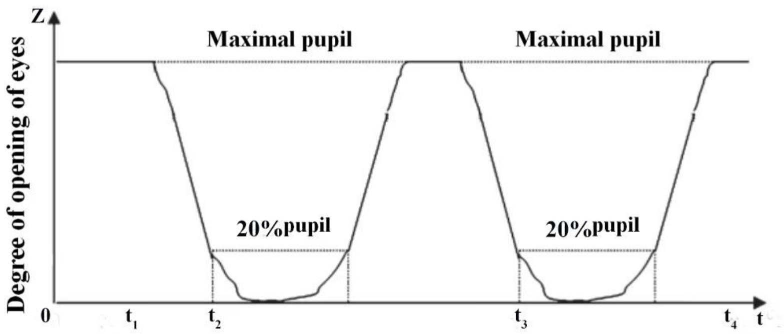

Figure 7. Schematic diagram of blink frequency detection algorithm.

$$f = \frac{c}{t_4 - t_1} \tag{1}$$

4. Hardware circuit design

OpenMV as an open source and low-cost machine vision module, provides rich machine vision development modules and rich functional interfaces through MicroPython language at the software level, which enables developers to quickly realize software development and debugging, and it is more convenient to obtain image information and control peripheral devices. The OpenMV4 version, equipped with ARM Cortex M7 STM32H743VI processor, has a high-frequency main processor, provides a variety of common interfaces in order to communicate with external MCUs, and also supports a variety of camera modules and real-time image transmission, which provides a good hardware support for the realization of the face positioning and fatigue detection system.

The MSP430F5529 is a chip based on the MSP430 microcontroller architecture, which has a built-in MSP430 core with 16-bit RISC architecture for fast operation and effective reduction of power consumption. It also includes a variety of standard interfaces such as UART, I^2C, SPI, etc., which facilitates communication with external devices.

OpenMV's P5, P4 pins are connected to the MSP430F5529 microcontroller's P3.3, P3.4, P7 connects to the PWM signal terminal of the pan servo, P8 connects to the PWM signal terminal of the tilt servo. 3.3V, GND are connected to the MSP430F5529 microcontroller's 3.3V, GND.

MSP430F5529 through the hardware I^2C bus interface P4.1, P4.2 and the I^2C bus type E^2PROM memory module AT24C512 SDA, SCL connected, AT24C512 has 512KB of storage space for storing special road information, when the MSP430F5529 read the positioning module information and the storage of special road position When MSP430F5529 reads the information of the positioning module and the stored special road condition location information, it triggers the sound and light alarm to remind the driver to pay more attention; the SDA and SCL of the I^2C OLED are connected to the P3.0 and P3.1 of the MSP430F5529 to realize the data communication of the I^2C bus mode through the software configuration; the positioning module adopts the serial communication, and the TXD and RXD of the transmit and receive bits are connected to the P2.3 of the MSP430F5529, P8.1 of the MSP430F5529, using an ordinary port to simulate the serial port to achieve data transmission. Alarm circuit is driven by a PNP-type transistor, P3.7 connected to the transistor base, when the control terminal P3.7 is a low level, the transistor saturated conduction, the buzzer alarm, when the base is extremely high level, the transistor cutoff, the buzzer to stop the alarm; LED using the current-flooding driver, P8.2 is a low level, the LED light, high level when the LED is extinguished. The specific hardware circuit is shown in the figure below. The whole system uses external DC 5 V power supply, the specific circuit shown in **Figure 8**.

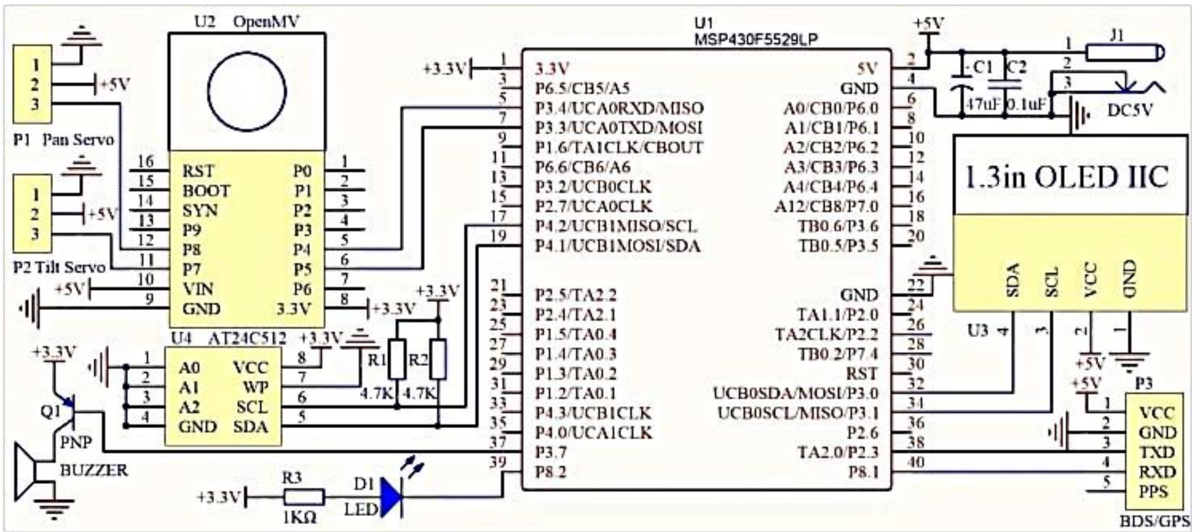

Figure 8. System hardware circuit diagram.

5. Software design

5.1. Software architecture

The software of the system consists of two parts. One is the image recognition and processing program running on the OpenMV main controller, which realizes face tracking, fatigue monitoring and communicates with the MSP430F5529 microcontroller. The second is the monitoring program downloaded in the MSP430F5529 microcontroller, which mainly receives the signal of blinking frequency, display, alarm, and real-time comparison of positioning information and stored information. The general structure of the software is illustrated in **Figure 9**.

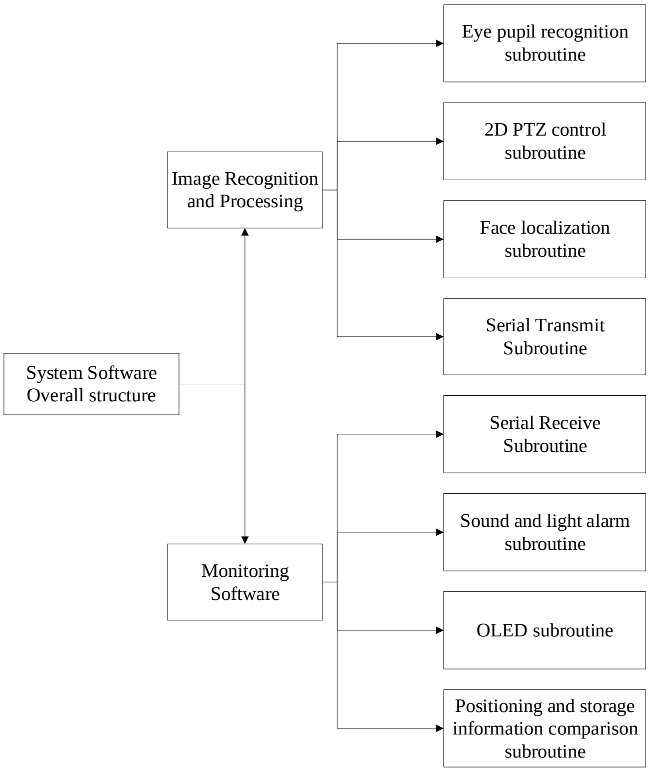

Figure 9. Overall software structure of the system.

5.1.1. OpenMV face localization software design

Face localization is mainly realized by OpenMV camera and two servos in hardware, and its flowchart is shown in **Figure 10**.

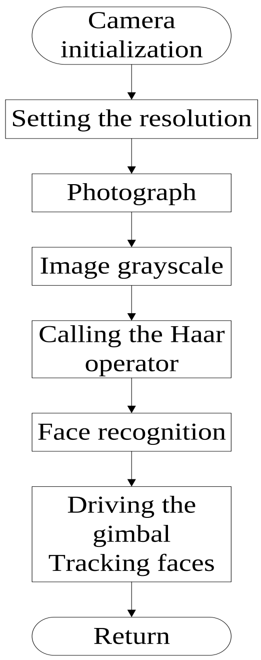

Figure 10. Flowchart of face positioning software.

First the camera is initialized, the resolution of the OV5640 camera is adjusted to be able to achieve a frame rate of 60 FPS, and a single frame image is captured after completing the camera settings. The captured color image is converted into a grayscale map as a preprocessing part of image processing. Load the Haar operator of the face to recognize the grayscale map, if the recognition is successful, the system generates a rectangular tuple (x,y,w,h) containing the position and size information of the face. If the recognition is not successful, the system returns an empty tuple, i.e., the driver is not found. Then, based on the rectangular tuple of face position and size (x,y,w,h), the deviation is calculated and fed back to the servo controlling the gimbal, so as to adjust to the angle that keeps the face in the center of the screen [29,30].

5.1.2. OpenMV pupil recognition software design

The program flow for implementing pupil recognition for OpenMV in this design is shown in **Figure 11**.

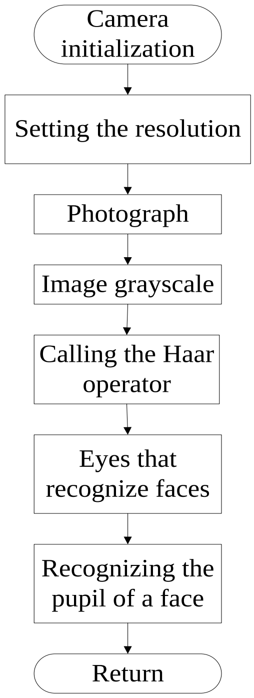

Figure 11. Pupil recognition flowchart.

Before image processing, the camera is first reset and its contrast and gain are set. The resolution of OV5640 is adjusted to 640 × 480. after completing the setup, the camera is operated to take an image frame, the color photograph taken is converted into a grayscale map, the Haar operator of the human eye is used to locate the human eye in the grayscale map, and if successful, a rectangular tuple representing the position and size of the eye (x,y,w,h) is obtained, otherwise an empty tuple is returned.

Based on the specific size and location information of the eye region, the darkest part of the color is retrieved to determine the pupil location, if the location and size of the pupil is detected, the recognition is successful, if an empty tuple is returned, the recognition process fails. Assuming that the driver is blinking, after completing a pupil detection cycle, the obtained pupil position and size information is analyzed to determine whether the detection was successful or failed. An empty return result means that the pupil was not recognized and it is assumed that the driver is in the blinking period. By monitoring the number of times a driver blinks in a given period of time, it is possible to assess whether he or she is at risk of driving fatigue [31].

5.1.3. Pupil recognition to determine fatigue driving monitoring software design

Usually the normal blinking frequency range for adults is 16 to 20 times/min, each lasting about 0.3 s. In the state of driving fatigue, the blinking frequency will rise. Studies have shown that the blinking frequency increases when drivers drive continuously for a long period of time and their fatigue level deepens, and when the frequency rises to 30 times/min, an obvious fatigue signal will appear. Therefore, in order to accurately determine whether a driver is fatigued or not, the blinking frequency is set at 30 times/min as the critical criterion for fatigue. Under normal circumstances, the length of a human's blinking and closing time is about 0.2 to 0.8 s. Taking this physiological feature into account, the system is unable to detect the pupil during the 0.8-s time period, and the system recognizes this as a complete blinking action and counts it.

5.1.4. Design of auxiliary module for cervical lumbar EMG analysis

In order to further supplement the existing fatigue driving detection system, the study introduced the neck and waist EMG analysis from the perspective of biomechanics to evaluate the fatigue state of drivers more comprehensively. The muscle activity of the neck and waist is closely related to the driver's posture and fatigue, especially during a long driving process, the muscle fatigue of the neck and waist will significantly affect the driver's reaction ability and attention. The use of surface myoelectric sensors (sEMG) attached to the driver's neck and lower back key muscle groups, these muscles are prone to fatigue during prolonged driving, and their activity can reflect the fatigue of the driver. The sensor wirelessly transmits the collected EMG signals to OpenMV for real-time processing and analysis. The collected EMG signal is first filtered to remove high-frequency noise and low-frequency drift. The filtered signal is rectified and smoothed to obtain the envelope of muscle activity, which is convenient for subsequent feature extraction. Multiple time-domain and frequency-domain features were extracted from the pre-processed EMG signals to reflect the intensity and fatigue of muscle activity. The extracted EMG features were compared with the preset fatigue thresholds. When the fatigue index of the neck and waist muscles exceeds the set threshold, the system determines that the driver is in a state of fatigue. The results of EMG signal analysis were fused with the existing blink frequency and facial positioning data, and the fatigue state of drivers was evaluated comprehensively by multi-modal data fusion algorithm.

6. System testing

6.1. Face recognition test gimbal positioning

The recognition effect of the face after changing the light intensity is shown in **Figures 12** and **13**.

Figure 12. Face recognition test chart under strong light without glasses.

Figure 13. Face recognition test chart under bright light with glasses.

When executing the actual driver facial positioning test, the OpenMV camera is first connected to the two servos of the gimbal, and then connected to the PC, and the facial positioning subroutine is loaded and debugged through the OpenMV IDE. Under the condition that the camera captures the face, the head moves along the horizontal direction with different speeds, and the deviation and control output adjustment values of the horizontal servos change in real time. The deviation and output data sent from the serial port are shown in **Figure 14**.

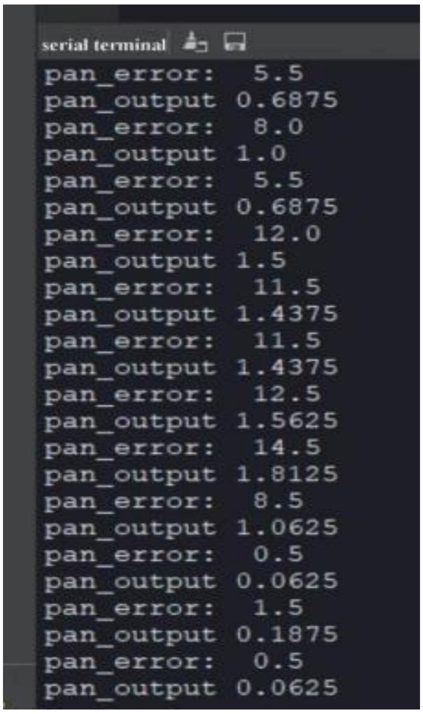

Figure 14. Face level moving servo deviation and output parameter.

The control period of the servo is 20 ms, and a dual-channel oscilloscope is utilized for observation, and the PWM waveforms of the horizontal servo and tilt servo are shown in **Figure 15** when the face moves. By verifying the data sent from the OpenMV integrated development environment (IDE) serial terminal and against the response actions of the servos, the results show that the subroutine for face localization is able to quickly track and locate the position of the face once it enters the field of view of the camera and moves.

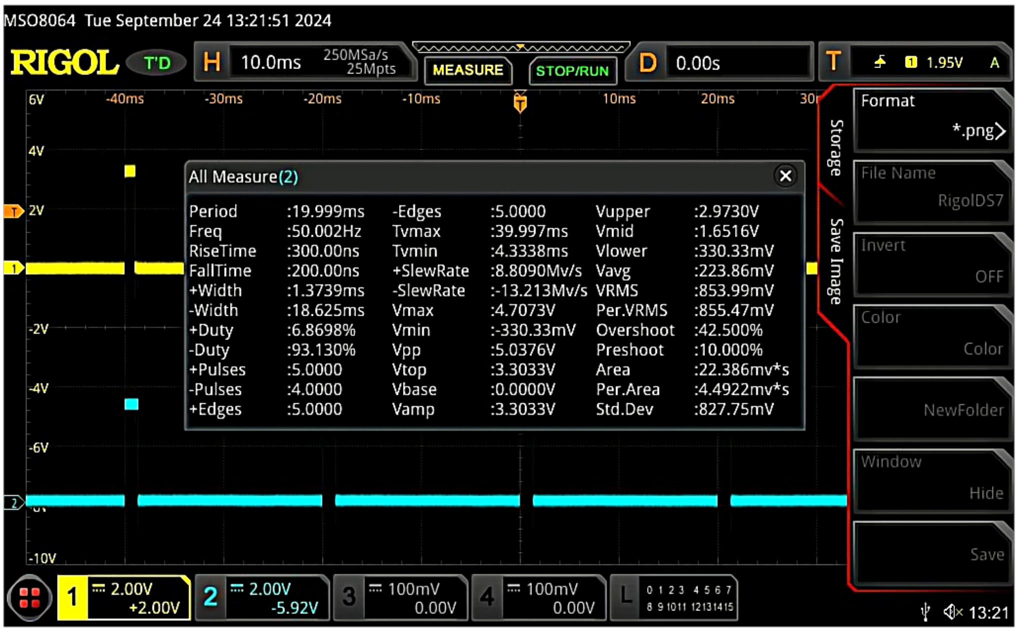

Figure 15. Oscilloscope observation of face-moving horizontal and tilting.

When conducting a PTZ face tracking experiment, the delay is quantified by measuring the time from the PTZ capturing the target to accurately targeting the target face. Experiments show that the average tracking delay of PTZ is 400 ms when PID parameters are not adjusted, and the delay can reach 600 ms when facing fast head movement, showing a significant lag. The effect of PID tuning: The adjusted system is more responsive, and the average tracking delay is reduced to about 250 ms. In the case of rapid head movements, the tracking delay is also kept to less than 350 ms, greatly reducing lag. It shows that the improved PID adjustment process improves the real-time tracking ability of PTZ, and makes PTZ more stable and efficient in the complex scene.

6.2. Human eye recognition and fatigue detection

6.2.1. Human eye recognition detection

In a bright light environment, the pupil of the left eye without glasses is recognized, as shown in **Figure 16**. Pupil recognition of the left eye wearing glasses in a bright light environment, as shown in **Figure 17**.

Figure 16. Left eye recognition test chart in bright light without glasses.

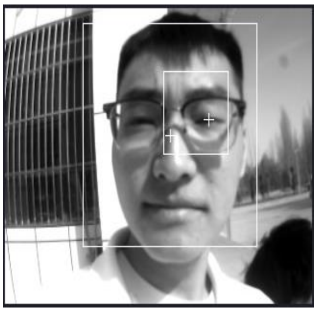

Figure 17. Left eye recognition test plot under bright light with glasses.

Regardless of whether the driver is wearing glasses or not, with or without glare, as long as both eyes are in the detection area of the camera to make any movement, the pupil recognition subroutine can quickly and accurately capture the human eye and its pupil position, at this time will be in the IDE interface with a square box marked with the human eye.

6.2.2. Fatigue detection

Before implementing the blink frequency measurement experiment, OpenMV's pupil tracking function should be calibrated for accuracy. Configure the OpenMV hardware, start the pupil recognition subroutine with image frame buffer, ensure that the eye moves left and right within the camera field of view, and at the same time manually record the number of blinks to calculate the blinking frequency and compare it with the data automatically measured by the system. The test of the system blink frequency is a dynamic measurement process, **Table 1** counts the number of blinks and the actual blink frequency that appear most frequently in the system blink frequency within 1 minute and the microcontroller determines whether it is fatigued or not.

Table 1. Sampling table for blink frequency measurements.

System blink frequency (cycles/min)	Actual blinking frequency (cycles/min)	Does the system determine fatigue	Experimental time
15	15	No	12:00–12:01
25	25	No	12:05–12:06
35	35	Yes	12:10–12:11
60	60	Yes	12:15–12:16
15	15	No	12:20–12:21
25	25	No	12:25–12:26

Table 1. (*Continued*).

System blink frequency (cycles/min)	Actual blinking frequency (cycles/min)	Does the system determine fatigue	Experimental time
35	35	Yes	12:30–12:31
56	60	Yes	12:35–12:36
15	15	No	12:40–12:41
25	25	No	12:45–12:46
34	32	Yes	12:50–12:51
57	60	Yes	13:00–13:01

In **Table 1**, there are some deviations between the System blink frequency and the Actual blinking frequency. The main sources of deviations are detection limitations, hardware limitations and external factors. The system may miss part of the blinking action during rapid blinking, especially at higher frequencies. Moreover, the processing speed of the main control chip STM32H743 may cause that the detection of rapid blinking is not completely accurate. When some special lighting changes or interference actions appear, the recognition accuracy of the camera may also be affected. In the EMG analysis experiment, the EMG signal is filtered to remove high-frequency noise and low-frequency drift, and then the envelope signal of muscle activity is extracted by rectification and smoothing. Muscle fatigue was evaluated by extracting time-domain and frequency-domain features from the processed signals. During the experiment, different fatigue thresholds were set. When the muscle fatigue index exceeded the threshold, the system would detect the fatigue state of the driver. The results of the experiment showed that after more than 90 min of continuous driving, the EMG in the neck and waist showed clear signs of fatigue. Specifically, the average frequency of activity of the filtered trapezius muscle in the neck increased from 0.5 Hz under normal conditions to 0.8 Hz under fatigue conditions, and the frequency of activity of the lumbar erector spine muscle also increased from 0.4 Hz to 0.7 Hz. At this time, the system detects that the fatigue index of the electromyographic signal exceeds the preset threshold, and the fatigue alarm is issued. In addition, combined with the blink rate and facial positioning data, the system's judgment accuracy reached more than 95% under fatigue. By combining neck and waist EMG with eye blink frequency, the experimental results show that the introduction of EMG significantly improves the detection accuracy of tired driving. Compared with relying solely on blink frequency, the added auxiliary module improves the overall evaluation ability of the system for driver fatigue state. These data fully verify the effectiveness of the EMG analysis module in practical applications.

6.3. Complex scene testing

In order to verify the robustness of the system under different lighting environments, four tests of typical complex lighting scenarios were added. The low light environment at night is 50 Lux, simulating night driving without street lights. The strong backlight environment is 1000 Lux, simulating direct sunlight or direct headlights. Dynamic shadow interference is a periodic change in light intensity between 200 and 800 Lux, simulating the occlusion of trees or buildings. The hybrid light environment consists of headlights, street lamps and natural light with a light intensity of 300–600 Lux. Use the camera resolution of 640 × 480, frame rate of 60 frames per second, dynamic exposure adjustment is enabled. The test subjects were 10 drivers, five of whom wore glasses and five without glasses, and each driver was tested three times in each environment. Test results of complex scenarios are shown in **Table 2**.

Table 2. Test results of complex scenarios.

Test scenario	Facial positioning success rate (%)	Accuracy (95% CI)	Pupil recognition accuracy (%)	Average response time (ms)	Fatigue detection false alarm rate (%)
Low light at night	93.3	91.2–94.1	88.6	210	4.2
Strong backlight environment	87.5	86.5–88.3	82.4	230	6.8
Dynamic shadow jamming	91.0	90.2–92.1	85.1	195	5.5
Mixed light environment	95.6	93.7–96.6	90.2	185	3.7

As can be seen from **Table 2**, the system dynamically improves the camera gain, and the success rate of facial positioning is maintained at 93.3%, while the false positive rate is relatively low (4.2%), mainly due to the loss of some frames in the blink action under low light. The backlight reduced the contrast of the face area, and the localization success rate dropped to 87.5%. Through the adaptive threshold adjustment of Haar classifier, the pupil recognition accuracy is still 82.4%. In dynamic shadow interference, the system compensates for light mutation by fast interframe difference method, the response time is reduced to 195 ms, and the performance is better than static environment. Experiments show that the system can maintain high precision and real-time performance under complex lighting conditions, especially in dynamic shadow and mixed light scenes. Through dynamic exposure adjustment, Haar classifier optimization and multi-modal data fusion, the interference of ambient light on fatigue detection is significantly reduced, and the robustness and practicability of the design scheme are verified. To further ensure the superiority of the research method. This study introduces the current mainstream Method based on convolutional neural network and Traditional Face Localization in Mixed light environment for comparison. As shown in **Table 3**.

Table 3. Comparison of fatigue detection algorithms.

Algorithm	Accuracy (%)	Mean Squared Error (MSE)	Confidence Interval (95% CI)	Speed (ms per frame)	False Alarm Rate (%)
Research method	95.6	0.01	93.7–96.6	185	3.7
Method based on convolutional neural network	89.5	0.03	87.0–92.0	250	5.5
Traditional Face Localization	93.3	0.02	91.2–94.1	210	4.2

As can be seen from **Table 3**, in terms of accuracy, 95.6% of the research Method is higher than 89.5% of the Method based on convolutional neural network and 93.3% of the Traditional Face Localization. And the research method has faster computational efficiency, becoming the only one that takes less than 200 ms. It shows that the research method has stronger performance in complex environment. In the same scene for a long time test, within 6 h, the system's face positioning accuracy has been maintained at more than 92%, and the blink frequency detection accuracy has reached 96%. In addition, the system's response time is maintained at around 210 ms, ensuring real-time performance. During the whole experiment period, the false positive rate of the system is only 3.8%, showing good stability. In the simulated fatigue driving scenario, when the driver's blink frequency reaches 30 times/min, the system accurately determines the fatigue state and issues an alarm in time. These data prove the effectiveness and stability of the research method in long-term driving, and it is suitable for fatigue detection in practical driving scenarios.

7. Conclusion

Because the pupil is small, to improve the detection distance can choose a telephoto lens, the design tries to increase the LCD on top of OpenMV, but it reduces the real-time graphics acquisition. This design takes light weight, real-time and high precision as the design index, compares the advantages and disadvantages of traditional machine vision detection methods in fatigue driving, and proposes a design scheme of face positioning and fatigue driving detection system based on OpenMV and microcontroller. According to the proportion of eye closure of the driver during driving, fatigue driving is judged. The information of the driver's lumbar muscles is analyzed through the neck and lumbar EMG to provide assistance for the system judgment. The positioning information is obtained through the positioning module, and is compared with the information prone to traffic accidents in the storage module to provide the driver with the function of road condition prediction and alarm. The system adopts OpenMV image processing module, whose onboard camera and supported firmware make the development easy and fast. Optimized for master-slave mode, the system combines the advantages of high efficiency and high functionality, which helps to improve driving safety. However, the research method also has some limitations. The low hardware performance may limit the complexity and real-time processing ability of the algorithm in the long run. Complex road conditions and individual differences of drivers make it difficult for the system to provide a unified fatigue detection standard, and more personalized adjustments are needed. The system also faces integration difficulties and costs, especially when embedded and deployed in existing vehicle electronic systems. Therefore, although the system has the potential to improve driving safety, the above problems still need to be solved in practical applications to improve its reliability and practicality.

Author contributions: Conceptualization, PZ and YJ; methodology, PZ; software, YJ; validation, PZ, YJ and YZ; formal analysis, PZ; investigation, YZ; resources, PZ; data curation, PZ; writing—original draft preparation, PZ; writing—review and editing, YJ; visualization, YZ; supervision, YJ; project administration, PZ; funding acquisition, PZ. All authors have read and agreed to the published version of the manuscript.

Acknowledgments: "Tianchi Talent" Introduction Plan Funding Project.

Ethical approval: Not applicable.

Conflict of interest: The authors declare no conflict of interest.

References

1. Zhang A, Li Q, Li Z, Li J. Multimodal fusion convolutional neural network based on sEMG and accelerometer signals for intersubject upper limb movement classification. IEEE Sensors Journal. 2023; 23(11): 12334–12345.
2. Salah M, Ayyad A, Ramadan M, et al. High speed neuromorphic vision-based inspection of countersinks in automated manufacturing processes. Journal of Intelligent Manufacturing. 2024; 35(7): 3067–3081.
3. Yang H, Liu L, Min W, et al. Driver yawning detection based on subtle facial action recognition. IEEE Transactions on Multimedia. 2020; 23: 572–583.
4. Bai J, Yu W, Xiao Z, et al. Two-stream spatial–temporal graph convolutional networks for driver drowsiness detection. IEEE Transactions on Cybernetics. 2022; 52(12): 13821–13833.
5. Ansari S, Naghdy F, Du H P. Driver mental fatigue detection based on head posture using new modified ReLU-BiLSTM deep neural network. IEEE Transactions on Intelligent Transportation Systems. 2022; 23(8): 10957–10969.
6. Brar DS, Kumar A, Mittal U, et al. Face detection for real world application. In: Proceedings of the 2021 2nd International Conference on Intelligent Engineering and Management (ICIEM); 28–30 April 2021; Moscow, Russia; pp. 239–242.
7. Wang R, Qin JM. Fuzzy PID control method of air conditioning supply air temperature based on multi-sensing features fusion (Chinese). Chinese Journal of Sensors and Actuators. 2023; 36(6): 943–948.
8. Xu Y, Yan W, Yang G, et al. CenterFace: Joint face detection and alignment using face as point. Scientific Programming. 2020; (2): 1–8.
9. Liu Y, Deng J, Wang F, et al. DamoFD: Digging into Backbone Design on Face Detection. In: Proceedings of the Eleventh International Conference on Learning Representations (ICLR); 1–5 May 2023; Kigali, Rwanda.
10. Praveen KS, Kesava JV, Subramanya V, et al. A multiple face recognition system with dlibs resnet network using deep metric learning. Journal of Critical Reviews. 2020; 7(6): 856–859.
11. Wang X, Zhang S, Wang S, et al. Mis-classified vector guided softmax loss for face recognition. In: Proceedings of the AAAI Conference on Artificial Intelligence; 7–12 February 2020; New York, USA. pp. 12241–12248.
12. Cai M, Cheng N, Cao C, et al. Adaptive hardness indicator softmax for deep face recognition. International Journal of Pattern Recognition and Artificial Intelligence. 2022; 36(4).
13. Kim M, Jain A K, Liu XM. Adaface: Quality adaptive margin for face recognition. In: Proceedings of the IEEE/CVF Conference on Computer Vision and Pattern Recognition; 18–24 June 2022; New Orleans, LA, USA. pp. 18750–18759.
14. El-Nabi SA, El-Shafai W, El-Rabaie ESM, et al. Machine learning and deep learning techniques for driver fatigue and drowsiness detection: A review. Multimedia Tools and Applications. 2024; 83: 9441–9477.
15. Zhou Y, Zeng CQ, Mu ZD. Optimal feature-algorithm combination research for EEG fatigue driving detection based on functional brain network. IET Biometrics. 2023; 12(2): 65–76.
16. Akrout B, Mahdi W. A novel approach for driver fatigue detection based on visual characteristics analysis. Journal of Ambient Intelligence and Humanized Computing. 2023; 14(1): 527–552.
17. Dogan S, Tuncer I, Baygin M, Tuncer T. A new hand-modeled learning framework for driving fatigue detection using EEG signals. Neural Computing and Applications. 2023; 35(20): 14837–14854.
18. Jiao Y, Chen X, Sun Z, et al. Data-driven detection and assessment for urban railway transit driver fatigue in real work conditions. Transportation research record. 2023; 2677(1): 1367–1375.
19. Yi Y, Zhou Z, Zhang W, et al. Fatigue detection algorithm based on eye multifeature fusion. IEEE Sensors Journal. 2023; 23(7): 7949–7955.
20. Saleem AA, Siddiqui HUR, Raza MA, et al. A systematic review of physiological signals based driver drowsiness detection systems. Cognitive neurodynamics. 2023; 17(5): 1229–1259.
21. Sharma S, Kumar V. Distracted driver detection using learning representations. Multimedia Tools and Applications. 2023; 82(15): 22777–22794.
22. Hussein RM, Miften FS, George LE. Driver drowsiness detection methods using EEG signals: A systematic review. Computer methods in biomechanics and biomedical engineering. 2023; 26(11): 1237–1249.
23. Tao K, Xie K, Wen C, He J. Multi-feature fusion prediction of fatigue driving based on improved optical flow algorithm. Signal, Image and Video Processing. 2023; 17(2): 371–379.

24. Min J, Cai M, Gou C, et al. Fusion of forehead EEG with machine vision for real-time fatigue detection in an automatic processing pipeline. Neural Computing and Applications. 2023; 35(12): 8859–8872.
25. Yi Y, Zhang H, Zhang W, et al. Fatigue working detection based on facial multifeature fusion. IEEE Sensors Journal. 2023; 23(6): 5956–5961.
26. Lyu H, Yue J, Zhang W, et al. Fatigue Detection for Ship OOWs Based on input Data Features, from the Perspective of Comparison with Vehicle Drivers: A Review. IEEE Sensors Journal. 2023; 23(14): 15239–15252.
27. Sar I, Routray A, Mahanty B. A review on existing technologies for the identification and measurement of abnormal driving. International journal of intelligent transportation systems research. 2023; 21(1): 159–177.
28. Cheng W, Wang X, Mao B. A multi-feature fusion algorithm for driver fatigue detection based on a lightweight convolutional neural network. The Visual Computer. 2024; 40(4): 2419–2441.
29. Pan L, Yan C, Zheng Y, et al. Fatigue detection method for UAV remote pilot based on multi feature fusion. Electronic Research Archive. 2023; 31(1): 442–466.
30. Lu Y, Liu C, Chang F, et al. JHPFA-Net: Joint head pose and facial action network for driver yawning detection across arbitrary poses in videos. IEEE Transactions on Intelligent Transportation Systems. 2023; 24(11): 11850–11863.
31. Kumar V, Sharma S, Ranjeet. Driver drowsiness detection using modified deep learning architecture. Evolutionary Intelligence. 2023; 16(6): 1907–1916.